ISBN: 978-3-95450-231-8 ISSN: 2673-5490 doi: 10.18429/JACoW-IPAC2023-TUPM125

STATUS OF THERMOMECHANICAL STUDIES OF THE SIS100 EMERGENCY BEAM DUMP SYSTEM

P. Drechsel*, R. Martin, O. Boine-Frankenheim, K. Knie, D. Ondreka
GSI Helmholtzzentrum für Schwerenforschung, Darmstadt, Germany

Abstract

The heavy ion synchrotron SIS100 is the flagship accelerator of the Facility for Antiproton and Ion Research (FAIR) currently under construction at GSI, Darmstadt. It will provide high intensity beams of particles ranging from protons to uranium ions at beam rigidities up to 100 Tm. Part of the machine protection system is an emergency beam dump that is partly inside the vacuum system and partly outside. The wide range of particles means that all components of the dump system are potentially exposed to high energy deposition densities at short time scales. The resulting shock waves are challenging for the mechanical stability of the components, including the vacuum window between inner and outer part of the dump. In this paper we present the status of thermomechanical simulations regarding the response of dump components to the most challenging beam impact scenarios. A first adaption to the vacuum window is assessed regarding it's potential to mitigate risks of failure.

INTRODUCTION

Beam intercepting devices (BIDs) have very high requirements to withstand thermal shock and irradiation during accelerator operation [1]. In this paper the components of the SIS100 emergency beam dump are examined. These BIDs are exposed to challenging impact scenarios. To estimate their performance, thermomechanical finite element method (FEM) analysis is performed within ANSYS®'s commercial FEM software. Linear-elastic material such as isotropic SIGRAFINE® R6650 and orthotropic Novoltex® SEPCARB® are simulated with the implicit solver of ANSYS® Mechanical™ 19.2. Hydrodynamic simulations of non-linear materials such as DENSIMET®185 and Ti6Al4V are solved within the explicit environment of ANSYS® Autodyn® 19.2. Thermal and mechanical limits are compared to the simulated dynamic response of the materials induced by ion beam impacts.

DEGRADER AND CARBON BLOCKS

In order to perform simulations on the thermomechanical response of the BIDs, it is crucial to obtain a map of the energy deposition that arises from the ion-matter interaction. These energy deposition maps are calculated by using Monte Carlo simulations. The code used is FLUKA [2–4]. Afterwards a transient thermal analysis within ANSYS® Mechanical™ is performed to calculate the temperature increase in the components during and after the ion beam pulse. As a final step a transient structural analysis is executed to simulate the beam-induced dynamic response. The simulation set-up is a weakly coupled thermoelastic problem, which means that the temperature variations influence the strain field but not vice-versa. Figure 1 shows a schematic of the different components of the SIS100 emergency beam dump. Two blocks consisting of graphitic materials with a length of 150 mm are inside the vacuum system. A degrader of the same material and a length of 7.5 mm will be placed 3.5 m upstream of the first carbon block to broaden the transverse energy distribution. The most challenging beam impact scenarios for the degrader and the first carbon block are assumed to be an emergency beam dump of 5×10^{11} uranium ions U^{28+} with an energy of 2.7 GeV/u and 350 MeV/u, respectively [1]. Bunch length for both cases is 50 ns. To keep the energy deposition as low as possible while still maintaining enough stopping power densities of degrader and beam dump are adjusted to be 1.1 g/cm^3 and 1.5 g/cm^3, respectively.

Table 1: Thermal and mechanical material limits for SIGRAFINE® R6650 and Novoltex® SEPCARB® [6–8].

Material Property		SGL R6650	Novoltex® SEPCARB®
Temperature	K	3895	3895
Flexural Strength	MPa	67	186‖
			145⊥
Compressive Strength	MPa	150	138‖
			166⊥
max. Tensile Strain		0.0051	0.0051

Suitable material candidates for both the degrader and the first two beam dump blocks are SIGRAFINE® R6650 from SGL group and Novoltex® SEPCARB® from Ariane group. To evaluate their performance under ion beam impact a comparison between the isotropic and orthotropic graphite is drawn. Carbon-fibre reinforced graphite (CFC) is currently used as a absorber material in the primary and secondary collimators of the LHC [9]. Novoltex® SEPCARB® is going to be used in the collimators of the SPS to High-Luminosity LHC transfer lines at CERN [10]. This material consists of stacked layers of carbon punctured by carbon fibers, forming the third direction of reinforcement perpendicular through the stacked layers [11]. Therefore different material limits are achieved along different directions. Table 1 shows the thermal and mechanical material limits of SIGRAFINE® R6650 and Novoltex® SEPCARB® where ‖ defines the failure limits along the stacked layers and ⊥ shows the limits perpendicular to the stacked layers. Simu-

* P.Drechsel@gsi.de

ISBN: 978-3-95450-231-8 ISSN: 2673-5490 doi: 10.18429/JACoW-IPAC2023-TUPM125

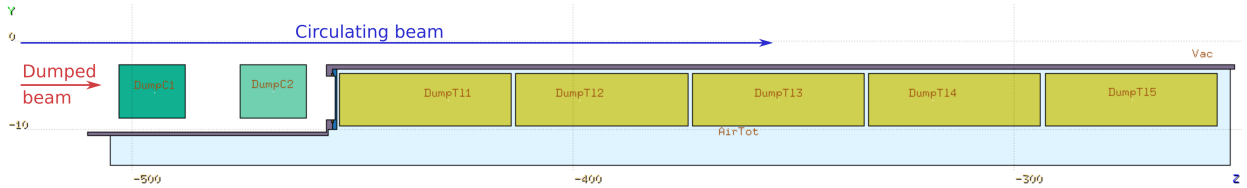

Figure 1: FLUKA model of the SIS100 beam dump [5]. The nominal beam is circulating at Y= 0. The dumped beam will be deflected downwards by kicker magnets located upstream and enter the carbon dump block (green) from the left. Low Z ion beams will exit through the vacuum window (blue) and enter the DENSIMET® 185 blocks (yellow) situated in air (blue) [1]. The degrader located 3.5 m to the left is not depicted.

lations of SIGRAFINE® R6650 quickly showed exceedance of material limits for degrader as well as beam dump. Material limits of Novoltex® SEPCARB® are higher compared to SIGRAFINE® R6650, therefore simulations are focused on the orthotropic behavior of Novoltex® SEPCARB® as it seems like a more promising candidate.

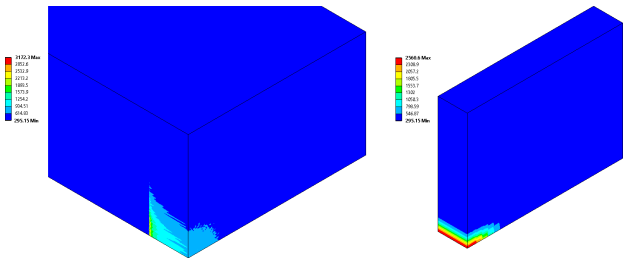

Figure 2: ANSYS® Mechanical™ quarter cut of temperature distribution of Novoltex® SEPCARB® beam dump (left) and degrader (right) after irradiation with 5×10^{11} uranium ions with an energy of 350 MeV/u and 2.7 GeV/u, respectively. Beam entering from the lower right.

Figure 2 shows the temperature distribution after beam impact with 5×10^{11} uranium ions U^{28+} for the first carbon block and the degrader. Peak temperature of 3172 K and 2516 K are reached inside the material, respectively. It can be seen that the full length of the degrader is penetrated by the uranium ion beam while most of the uranium ions are stopped inside the first carbon block at the Bragg-peak. The fast temperature increase inside the material causes the heated volume to rapidly expand. This causes compressive wave propagation which is reflected at the free surfaces. The resulting maximum compressive and tensile loads of the dynamic response are shown in Table 2. Thermal and mechanical material limits are not exceeded, compare with Table 1. Novoltex® SEPCARB® establishes a good performance under extreme thermomechanical loading. Degrader as well as both carbon blocks should be manufactured out the orthotropic graphite with an orientation of the carbon planes perpendicular to the direction of the beam. The reinforcement needling will then be parallel to the beam direction. The worst case scenarios studied in this paper were identified in [1] based on the assumption that peak energy deposition corresponds to the highest thermomechanical strain. Parameter scans of transverse distribution, beam intensity and ion energy suggest that this assumption is reasonable within realistic parameters. It is concluded that total energy deposition had little to no impact if the peak temperature was unchanged. However the results also suggest that transverse temperature gradients do play a role. Still we are confident that the beam impact scenarios studied here are representative of the strain the beam dump components must withstand.

Table 2: Thermal and mechanical results for graphite degrader and beam beam dump downstream irradiated with 5×10^{11} uranium ions with an energy of 2.7 GeV/u.

			Degrader	Dump
Temperature		K	2516	3172
Tensile Stress	∥	MPa	66	51
	⊥		26	7
Compressive Stress	∥	MPa	30	21
	⊥		40	38
Tensile Strain	∥		0.0018	0.0014
	⊥		0.0026	0.0006

TUNGSTEN BLOCKS

Similar to the simulation of the carbon materials in the previous chapter simulations regarding the DENSIMET®185 beam dump and the vacuum window are performed. Again an energy deposition map for the material is calculated by FLUKA Monte Carlo simulations. This energy deposition map is then applied as an internal energy load to the hydrocode of ANSYS® Autodyn® via an internal user subroutine. An explicit Lagrangian solver is used. The equation of state (EOS) of the materials and the strength model govern the dynamic response. For the materials the Mie-Grüneisen EOS [12] and the Johnson-Cook (JC) model [13] is used since the model is suitable for high temperatures and strain-rates.

The used material for the tungsten blocks is DENSIMET®185 [14, 15]. Protons will not be stopped in the carbon beam dump blocks due to the low density and stopping power. They are instead caught in the DENSIMET®185 blocks. The most challenging beam impact scenario is assumed to be an emergency beam dump of 2.5×10^{13} protons with an energy of 28.8 GeV and a bunch length of 50 ns [1]. For comparison the most critical ion beam is also simulated, 8.33×10^{11} xenon

ISBN: 978-3-95450-231-8 ISSN: 2673-5490 doi: 10.18429/JACoW-IPAC2023-TUPM125

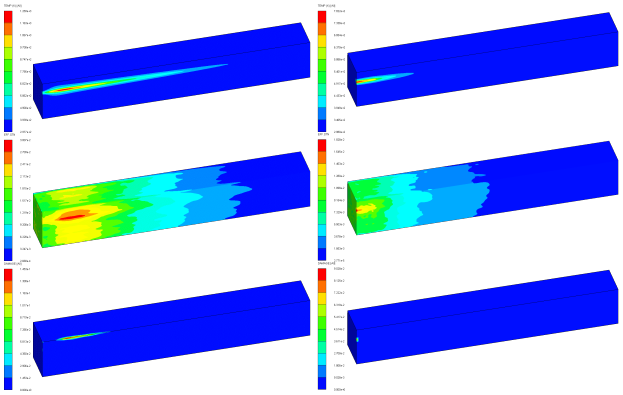

Figure 3: ANSYS® Autodyn® half cut of temperature distribution (top) of first DENSIMET®185 block after irradiation with 2.5×10^{13} protons with an energy of 28.8 GeV (left) and 8.33×10^{11} xenon ions Xe^{21+} with an energy of 3.9 GeV/u (right). Also shown are the effective strain (middle) and JC-damage (bottom) after 100 µs.

ions Xe^{21+} with an energy of 3.9 GeV/u and same bunch length. Thermal distribution for both cases is shown in Fig. 3. It can be seen that peak temperatures differ. Protons cause a thermal spike of 1267 K while xenon ions induce only 782 K. The penetration depth of protons is greater, therefore a larger volume is heated, which causes a different shock-wave to propagate into the material. For evaluation of the load onto the DENSIMET®185 block the damage from the cumulative JC-damage model is shown. The values can range from 0 to 1. Zero representing a material where no damage initiation occurred. After damage initiation the Young's modulus is reduced, modeling damage evolution by degradation of the material stiffness, leading to material failure at value 1 [16]. With an accumulated value of 0.1458 for protons and 0.0903 for xenon ions the load onto the beam dump can become critical after a single digit number of impacts since the cumulative damage model assumes no healing of the material. It can be seen that the area with the highest load is located in different areas for protons and xenon ions. While xenon ions induce the highest load at the entry point of the beam due to their lower energy deposition and penetration depth, protons cause the highest load on top of the beam dump. The greater temperature increase over a larger volume induces a massive compressive shock-wave which is then reflected to a tensile wave at the free wall of the beam dump. For protons the lion's share of the damage is induced by the first shock-wave.

VACUUM WINDOW

For the vacuum window the titanium alloy Ti6Al4V [17–19] is used. To perform hydrodynamic simulations within ANSYS® Autodyn® the geometry of the window has to be simplified. The 15 boreholes around the rim of the flange as well as chamfers could not be implemented without disturbing the internal user subroutine. An ion beam impact of 8.1×10^{11} tantalum ions Ta^{25+} with an energy of

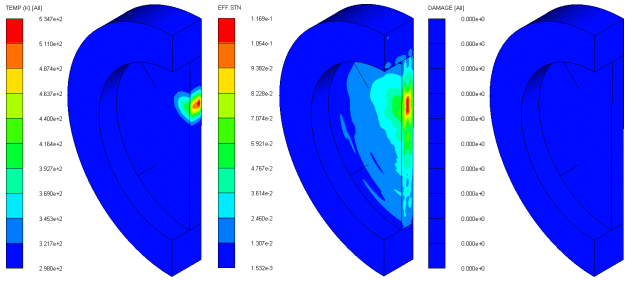

Figure 4: ANSYS® Autodyn® half cut of temperature distribution (left) of the Ti6Al4V vacuum window after irradiation with 8.1×10^{11} tantalum ions Ta^{25+} with an energy of 3.3 GeV/u. Also shown are the effective strain (middle) and JC-damage (right) after 100 µs.

3.3 GeV/u and a bunch length of 50 ns is expected to cause the highest load onto the material [1]. The design of the vacuum window allows an exchange if material fatigue is imminent.

Figure 4 shows the thermal and mechanical results of the hydrodynamic simulations of the Ti6Al4V flange with a wall thickness of 4 mm. Peak temperature after beam impact is 533 K. It can be seen that no damage occurs at all in the vacuum window. Due to the mechanical properties of the titanium alloy the flange only deforms elastically, therefore no plastic deformation can alter the material properties.

SUMMARY

The SIS100 emergency beam dump will be exposed to challenging beam impact scenarios. Numerical FEM analyses in both ANSYS® environments (Mechanical™ and Autodyn®) are a great tool to estimate the dynamic material response under these conditions. An analysis of different elements of the SIS100 beam dump is performed considering their individual challenges. Simulations show, that the installation of a degrader is crucial for the survivability of the graphite beam dump. For both beam dump components the material of choice will be a state of the art 3D-CFC. Ariane group's Novoltex® SEPCARB® establishes extraordinary material properties despite its orthotropy. Hydrodynamic simulations of the first DENSIMET®185 block show a critical load. It can be estimated that only a few proton beam impacts will cause fatal wear on the top of the beam dump. Since most of the damage is caused by the initial shock-wave being reflected off the free surface, finding optics that deflect the proton beam further downwards and increasing the distance to the top of the beam dump might reduce the mechanical load. If spatial constraints prevent any geometrical changes material substitution will be examined, e.g. changing the material in the front of the beam dump from DENSIMET®185 to Ti6Al4V. Future simulations will investigate this approach. The flange studies show that Ti6Al4V performs well under the irradiation with heavy ions. Temperature increases for tantalum ions Ta^{25+} is 235 K causing a pure elastic response. This is very favorable and reduces altering of material properties to a minimum.

ISBN: 978-3-95450-231-8 ISSN: 2673-5490 doi: 10.18429/JACoW-IPAC2023-TUPM125

REFERENCES

[1] R. Martin and D. Ondreka, "Challenges for the SIS100 Emergency Beam Dump System", presented at the 14th International Particle Accelerator Conference (IPAC'23), Venice, Italy, May 2023, this conference.

[2] https://fluka.cern

[3] C. Ahdida *et al.*, "New Capabilities of the FLUKA Multi-Purpose Code", *Frontiers in Physics*, vol. 9, p. 788253, 2022. doi:10.3389/fphy.2021.788253

[4] G. Battistoni *et al.*, "Overview of the FLUKA code", *Annals of Nuclear Energy*, vol. 82, pp. 10–18, 2015. doi:10.1016/j.anucene.2014.11.007

[5] V. Vlachoudis, "FLAIR: A Powerful But User Friendly Graphical Interface For FLUKA", *Advances in Space Research*, vol. 34, no. 6, pp. 1302–1310, 2004. doi:10.1016/j.asr.2003.03.045

[6] P. Simon *et al.*, "Dynamic Response of Graphitic Targets with Tantalum Cores Impacted by Pulsed 440-GeV Proton Beams", *Shock and Vibration*, vol. 2021, p. 1-19, 2021. doi:10.1155/2021/8884447

[7] F. Nuiry and A. P. Marcone, "Material Testing for Injection and Transfer Line Absorbers", in *Proc. 5th Joint HiLumi LHC-LARP Annual Meeting*, Geneva, Switzerland, 2015.

[8] J. Abrahamson, "Graphite Sublimation Temperatures, Carbon Arcs and Crystallite Erosion", *Carbon*, vol. 12, no. 2, p. 111-141, 1974. doi:10.1016/0008-6223(74)90019-0

[9] O. S. Bruening *et al.*, "LHC Design Report", CERN, Geneva, Switzerland, 2004. doi:10.5170/CERN-2004-003-V-1

[10] F. Nuiry *et al.*, "3D Carbon/Carbon composites for beam intercepting devices at CERN", *Material Design & Processing Communications*, vol. 1, no. 1, p. e33, 2019. doi:10.1002/mdp2.33

[11] A. Lacombe *et al.*, "3D Carbon-Carbon Composites are Revolutionizing Upper Stage Liquid Rocket Engine Performance by Allowing Introduction of Large Nozzle Extension", in *Proc. 50th AIAA/ASME/ASCE/AHS/ASC Structures, Structural Dynamics, and Materials Conference*, Palm Springs, USA, 2009. doi:10.2514/6.2009-2678

[12] O. Heuzé, "General form of the Mie–Grüneisen equation of state", *Comptes Rendus Mécanique*, vol. 340, no. 10, p. 679-687, 2012. doi:10.1016/j.crme.2012.10.044

[13] G. R. Johnson and W. H. Cook, "Fracture characteristics of three metals subjected to various strains, strain rates, temperatures and pressures", *Engineering Fracture Mechanics*, vol. 21, no. 1, p. 31-48, 1985. doi:10.1016/0013-7944(85)90052-9

[14] C. K. Sagar *et al.*, "Determination of Johnson Cook Material Model Constants and Their Influence on Machining Simulations of Tungsten Heavy Alloy", *Advances in Aerospace Technology*, vol. 1, p. 1-10, 2018. doi:10.1115/imece2018-88270

[15] The Plansee Group, https://www.plansee.com/.

[16] *ABAQUS Analysis User's Manual, Version 6.14*, Dassault Systèmes Simulia Corp, USA, 2014, http://130.149.89.49:2080/v6.14/pdf_books/ANALYSIS_2.pdf

[17] D. J. Steinberg, "Equation of State and Strength Properties of Selected Materials", LLNL, Livermore, USA, 1996.

[18] Y. Zhang *et al.*, "On the Selection of Johnson-cook Constitutive Model Parameters for Ti-6Al-4V Using Three Types of Numerical Models of Orthogonal Cutting", *Procedia CIRP*, vol. 31, p. 112-117, 2015. doi:10.1016/j.procir.2015.03.052

[19] M. Sbayti *et al.*, "Finite Element Analysis of hot Single Point Incremental forming of hip prostheses", in *Proc. NUMIFORM 2016: The 12th International Conference on Numerical Methods in Industrial Forming Processes* , Troyes, France, 2016. doi:10.1051/matecconf/20168014006